# BDH Final Project: Learning to Diagnose using Clinical Notes

**Jinmiao Huang**[1], **Cesar Osorio**[1], **Luke Wicent Sy**[1]
[1] **Georgia Institute of Technology, Atlanta, Georgia, USA**

**Abstract**

Clinical notes contain detailed interpretation of patients clinical information. The semantic analysis of such text is important and valuable in improving medical care systems. In this project, we apply deep learning based natural language processing frameworks to automatically assign clinical ICD-9 codes from those free-text clinical notes. Our best models are able to predict the top 10 ICD9 codes with 69.57% F1 and 89.67% accuracy (GRU); the top 10 ICD9 categories with 72.33% F1 and 85.88% accuracy (GRU); the top 50 ICD9 codes with 36.62% F1 and 91.48% accuracy (LR); the top 50 ICD9 categories with 43.01% F1 and 88.41% accuracy. A video summary of our work can be found at https://youtu.be/xHFYFPpXLUg. We made our evaluation tools and resources available at https://github.com/lsy3/clinical-notes-diagnosis-dl-nlp.

## 1 Introduction

Electronic health record (EHR) data capture variety of patient clinical information such as medical history, vital signs, lab test results, clinical notes, etc. EHR data build a continuous flow of information between the doctor and the patient. Clinicians can perform better diagnosis after a detailed understanding of the patient's medical history, disease progression and other symptoms and descriptions from clinic notes. Systematic reviews have shown the clinical care quality improvement using predictive analysis based on EHR data[1].

Some work use structured biosignal features in EHR to build the clinical decision making systems[2,3]. Others mining unstructured free-text to predict the diagnosis[4,5]. Consider the fact that more than 80% of all health record data is in unstructured text[6], these information contain detailed interpretation of the overall clinical information as well as big challenge in predictive analysis because of the unstructured nature. Thus, our work will mainly focus on exploring useful information from clinical notes and automatically assign diagnose codes (ICD-9) to the patient. Our goal is to develop an auto diagnostic system that learns from available EHR data, finds better disease or treatment progress patterns through statistical analysis, and provides optimal suggestions for clinical decision-making.

Recently, deep learning approaches have shown a significant improvement on many Natural Language Processing (NLP) tasks such as language translation, image caption and sentiment analysis. Deep learning models can often be trained end-to-end without any domain-specific and often tedious hand-designed feature engineering. Therefore, we will develop our diagnose learning system using the state-of-the-art NLP deep learning models.

Currently, there are two major categories of approaches for automatically assigning ICD-9 codes using text-free clinical notes. One is rule-based systems, the other one is machine learning-based methods. Rule-based systems are designed by human experts. This type of methods have out-performed other methods in many cases[7,8]. However, this kind of system heavily relies on the manual intervention of the medical professionals, thus hard to maintain and scale up to more general cases. Our work focuses on the machine learning-based automatic approach which do not require any domain knowledge from the medical experts. In this section, we will briefly review work in learning based approach.

Chen et al.[4] use semantics analysis method which includes dependency parsing of clinical records and the calculation of semantic matching score. There are also many research work on exploring traditional machine learning methods to clinical notes classification, such as Sequential Minimal Optimization[9], Support Vector Machine[10–13].

More recently, Nigam[14] applied deep learning techniques to classify ICD-9 code using clinical notes. Prakash et al.[5] used Condensed Memory Network with a pre-learned memory representation from a knowledge base (medical articles on Wikipedia) to do the same task.

## 2 Methodology

Figure 1 shows an overview of our methodology pipeline. Our methodology involves the following steps: data preprocessing, feature extraction, and lastly, model training and testing. Specifically, we ran the experiments using Azure virtual machines (NC24 with K80 GPU). Furthermore, spark was used for data preprocessing; Spark, sklearn, and gensim for feature extraction; and Spark ML, Keras, and Tensorflow for model training and testing. Section 2.1 to 2.3 describes each step in more detail. Each model is also evaluated under a set of metrics, as described in section 2.4.

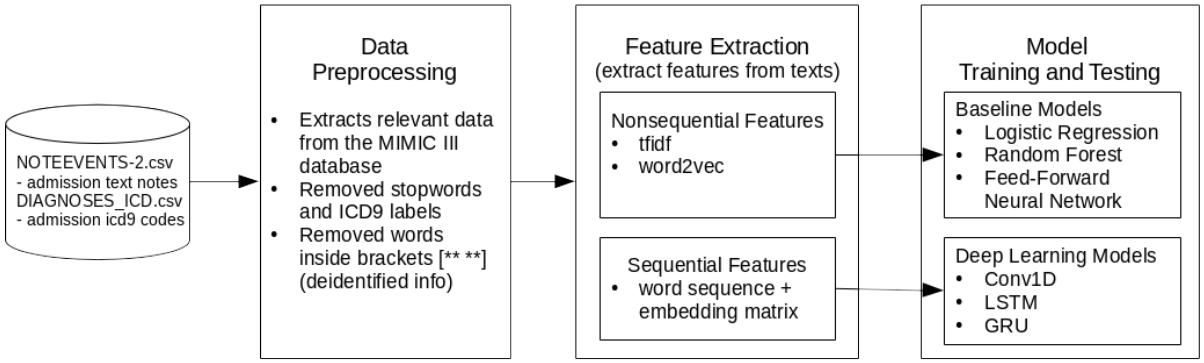


**Figure 1:** Methodology Pipeline Overview

### 2.1 Data Preprocessing

MIMIC III dataset is a large data set relating to patients admitted to critical care units at a large tertiary care hospital. It contains de-identified medical records of patients who stayed within the intensive care units at Beth Israel Deaconess Medical Center from 2001 to 2012[15]. The goal of this study is to explore useful semantic information using unstructured data, therefore only the free-text clinic note section from the dataset, specifically the *noteevents* table, was used. Furthermore, we focused on the *discharge summaries* category as it contains actual ground truth and free-text compared to other categories. This approach is similar to Prakash et al[5] . Since *discharge summaries* were written after the diagnosis was made, the notes are sanitized by removing any mention of class-labels (icd9 codes).

Table 1 describes the number of unique patients, hospital admissions, ICD9 codes and ICD9 categories involve in the MIMIC III dataset. *All MIMIC III* describes the whole dataset, while *noteevents* and *discharge summaries* describe the corresponding subsets.

| Coverage | Patients | Hospital Admissions | ICD9 Codes | ICD9 Categories |
|---|---|---|---|---|
| All MIMIC III | 46520 | 58976 | 6984 | 943 |
| *noteevents* | 46146 | 58361 | 6967 | 943 |
| *discharge summaries* | 41127 | 52726 | 6918 | 942 |

**Table 1:** MIMIC III Descriptive Statistics

The data was preprocessed to produce separate datasets through two approaches. The first approach is to treat the ICD-9 code independently from each other, find the admissions (unique HADM_ID) for each ICD-9 classification, and consider only records related to the top 10 and top 50 common ICD-9 codes. Top 10 and top 50 are chosen because they cover majority of the dataset (76.9% and 93.6% as can be observed in table 3, and for ease of comparison with the result of[14]. The second approach is to group ICD-9 codes into categories based on its hierarchical nature, with categories for larger sets of similar health conditions (e.g, "Cholera due to vibrio cholerae" has the ICD9 code 001.0, and is categorized as a type of Cholera, which in turn is a type of Intestinal Infectious Disease), and then find the patients for top 10 and top 50 common categories. Evaluation will be separately performed on the four datasets. The

four datasets will hereby be referred as *top-10-code*, *top-50-code*, *top-10-category* and *top-50-category* respectively.

Table 2 shows the top 10 ICD9 codes and top 10 ICD9 categories. Table 3 also describes the number of unique hospital admissions related to the four datasets mentioned in the earlier paragraph.

| ICD9 Code | Admissions |
|---|---|
| 4019: Hypertension | 20046 |
| 4280: Congestive heart failure | 12842 |
| 42731: Atrial fibrillation | 12589 |
| 41401: Coronary atherosclerosis | 12178 |
| 5849: Acute kidney failure | 8906 |
| 25000: Diabetes Type II | 8783 |
| 2724: Hyperlipidemia | 8503 |
| 51881: Acute respiratory failure | 7249 |
| 5990: Urinary tract infection | 6442 |
| 53081: Esophageal reflux | 6154 |

| ICD9 Category | Admissions |
|---|---|
| 401: Essential hypertension | 20646 |
| 427: Cardiac dysrhythmias | 16774 |
| 276: Disorders of fluid electrolyte | 14712 |
| 272: Disorders of lipoid metabolism | 14212 |
| 414: Other chronic ischemic heart disease | 14081 |
| 250: Diabetes mellitus | 13818 |
| 428: Heart failure | 13330 |
| 518: Other diseases of lung | 12997 |
| 285: Other and unspecified anemias | 12404 |
| 584: Acute kidney failure | 11147 |

**Table 2:** Top 10 ICD9

| Data Set | Hospital Admissions | *discharge summaries* Coverage (%) |
|---|---|---|
| *top-10-code* | 40562 | 76.93% |
| *top-50-code* | 49354 | 93.60% |
| *top-10-category* | 44419 | 84.24% |
| *top-50-category* | 51034 | 96.79% |

**Table 3:** Dataset Descriptive Statistics

The filtered datasets will be split to 50-25-25 for training, validation and testing.

### 2.2 Feature extraction

We use two approaches for feature extraction: term frequency - inverse document frequency (TF-IDF) and word2vec. We will use TF-IDF as a baseline, and compare the results to word2vec.

TF-IDF is intended to evaluate how important a word is to a document in a collection of documents or corpus. TF-IDF is the product of two statistics: TF and IDF. TF is the number of times a word appears in a given document and IDF measures whether a word is common or rare across the corpus. We use the following definition of IDF for our calculations:

$$IDF(w) = log\frac{N_d}{DF(d,w)} + 1$$

where $N_d$ is the total number of documents and $DF(d, w)$ is the number of documents that contain word w.

To calculate TF-IDF, first we tokenized all the notes in the filtered training data set, then create a document-word matrix with the count of each word in each note (TF) and finally multiply each word by the corresponding IDF. We used two TF-IDF configurations: (1) one with top 40,000 words with highest TF-IDF scores as the bag of word features and (2) a second one with minimum document frequency of 10 and maximum document frequency of 0.8, which reduces our total number of words to around 20,000 words.

word2vec[16,17] takes a tokenized text corpus as an input and produces word vectors as output. We used the Continuous Bag of Words (CBOW) architecture which predicts the target word based on the context: words that precede and follow the target word. CBOW is basically a feed forward neural net model (FFNN) that consists of inputs, projection and output layers where the traditional non-linear hidden layer is removed to reduce time complexity and the projection

layer is shared by all the words. The inputs are words in the context (see Figure 2). We use text notes from MIMIC III as corpus to train our word2vec model. We also use pre-trained word vectors induced from PubMed found on https://github.com/ cambridgeltl/BioNLP-2016[18]

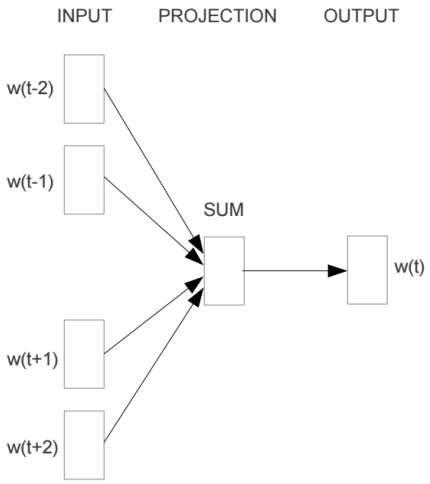


**Figure 2:** word2vec - CBOW architecture

### 2.3 Model Training and Testing

One fundamental assumption adopted by traditional supervised learning algorithms is that each sample has only one label assigned to it. In our problem, each sample has multiple (one or more) ICD-9 codes attached to it. Generally, there are two main methods for tackling the multi-label classification problem[19] (1) problem transformation methods and (2) algorithm adaptation methods. Problem transformation methods transform the multi-label problem into a set of binary classification or regression problems, multiple binary classifiers are trained separately for each label. Algorithm adaptation methods adapt the algorithms to perform multi-label classification in its full form and only one classifier are trained for all the labels.

In this study, we first create three baseline approaches: Linear Regression, Random Forests and Feed Forward Neural Network. Among which, we used problem transformation methods to get the multi-label output for Linear Regression and Random Forest classifiers. Specifically, in order to assign each sample a set of target labels, we simply trained $n$ different models for $n$ different labels, each model independently predicts a mutual exclusive output (0 or 1) for each sample data. For Feed Forward Neural Network, we used algorithm adaptation based methods, since neural network can be easily adapted to multi-label problem by setting up multiple neurons in the network output layer and set each neuron to a target label correspondingly. CNN, LSTM, and GRU also used algorithm adaptation based methods, similar to Feed Forward Neural Network. In this section, we will describe our implemented models in detail.

#### 2.3.1 Baseline Model: Logistic Regression

Our first baseline model is a binomial logistic regression model implemented using Spark ML. For each label (ICD-9 code or category), a separate logistic regression model was trained and each model independently predicts the said label (0 or 1 for the corresponding ICD-9 code or category). We tried different configurations; specifically "no. of iterations" was tuned between 5 to 100. Since we only use notes under *discharge summaries* category, there is 1 note per admission. Features are extracted from this note and are used as inputs for this classifier. For *tfidf*, the features are directly used as input features. For *word2vec*, the input features are the average of all the feature vectors of the words in the notes.

### 2.3.2 Baseline Model: Random Forest

Our second baseline model is a random forest model implemented using Spark ML. The same approach and input for the logistic regression were used here (one model for each label). Different configurations were also tried, specifically "tree depth" was tuned between 5 to 30.

### 2.3.3 Feed-Forward Neural Network

One advantage of Neural Network is that it can be fitted to multi-label problem in just one model with the proper activation function. We implement the feedforward neural network as the baseline for algorithm adaptation based (described in 2.3) multi-label classification problem. We use the same input features and train-test data split as previously described. We use ReLU activation function for all the hidden layers and sigmoid activation function for the output layer. We use binary cross entropy as the loss function and stochastic gradient decent as the optimizer. We tried several neural network models with one to four different hidden layers. For each hidden layer, we tried a combination of neuron size 50, 100, 300, 500 and 1000, a total of seven models. The results for different configurations are detailed in our attached spreadsheet *Experiments.xlsx*. The predicted label for each output is set to 1 for output probability greater than or equal to 0.5 and 0 otherwise. The best performance model is with three hidden layers with size 1000, 500, 100 respectively.

### 2.3.4 Convolutional Neural Network

Convolutional neural networks (CNN) have achieved remarkable results in image processing related problems. Images have the property of being "stationary", this suggests that the features that we learn at one part of the image can also be applied to other parts of the image[20]. Recently, CNN models have also shown excellent results for NLP such as in semantic parsing[21], search query retrieval[22], and sentence classification[23]. Thus we tested on a series of experiments with CNN for our problem.

The input features for this classifier are $N$ most recent word sequences (taken from the notes). If we don't have enough feature events, we pad zero vectors at the beginning. The word sequence is then converted into vectors using an embedding matrix based on a *word2vec* model. We tried three to ten convolutional layers with size 64, 128, 256 and one to three fully connected dense layers attached to the last convolutional layer with size 4096, 1024 and 128. Among our model architecture setting, the best performed model pipelines are shown in Figure 11 and 12. Under the hardware setting described, the training time for CNN is less than 30 minutes with 500 maximum epochs and early stop if the validation loss doesn't improve for consecutive 10 epochs.

### 2.3.5 Recurrent Neural Network, LSTM, and GRUs

Finally, we implement Recurrent Neural Networks (RNNs), Long Short Term Memory (LSTM) networks and Gated Recurrent Units (GRUs) using Keras with Tensorflow backend. The input features is the same as we used in CNN. We tried up to three stacked recurrent layers with a combination 64, 128 and 256 units for each layer in our RNNs. We used the well-known LSTM and GRU units for our RNNs. To predict the ICD-9 classification, we only consider the output nodes of the last time step, and apply the same activation function and loss function as we choose for Feed-Forward Neural Network. The best performed mode architecture for LSTM and GRU are shown in Figure 9 and 10. Under the specified hardware setting, the training time for LSTM and GRU is about 6 to 18 hours with 200 maximum epochs and early stop if the validation loss doesn't improve for consecutive 5 epochs.

## 2.4 Metrics

Combinations of our dataset, feature extraction methods, and models are evaluated under different performance metrics, including precision, accuracy, F-score and recall metrics for multi-label classification. Specifically, the following

metrics are used[24]:

$$\text{Precision} = \frac{1}{n}\sum_{i=1}^{n}\frac{|Y_i \cap Z_i|}{|Z_i|} \qquad \text{Recall} = \frac{1}{n}\sum_{i=1}^{n}\frac{|Y_i \cap Z_i|}{|Y_i|}$$

$$F_1 = \frac{1}{n}\sum_{i=1}^{n}\frac{2|Y_i \cap Z_i|}{|Y_i| + |Z_i|} \qquad \text{Accuracy} = \frac{1}{n}\sum_{i=1}^{n}\frac{|Y_i \cap Z_i|}{|Y_i \cup Z_i|}$$

$$AUC_{macro} = \frac{1}{q}\sum_{j=1}^{q} AUC_j$$

$$\textit{Hamming Loss} = \frac{1}{q}\sum_{i=1}^{q}\frac{xor(Z_i, Y_i)}{n}$$

where $Y_i$ is the set of predicted labels, $Z_i$ is the set of ground truth labels, and $n$ is the number of samples. $q$ is the number of total samples. $AUC_{macro}$ is the macro average of Area Under the Curve (AUC).

We observed there is a highly imbalanced relation between non-diagnose and diagnose observations (80/20 or more for most cases). Therefore, the relative high score in some metrics do not indicate the models worked well enough for this task. For example, the performance for a model with all the test samples labeled as non-diagnose (model only predicts zeros or no disease for all the test patients) is presented in table 4. We can see that the accuracy, AUC macro and Hamming loss have non-zero values. Accuracy in particular has high values. Therefore, we focus on improving the performance of the initial zero entries in table 4 (Precision, Recall, and F1) and also recorded accuracy as a casual reference.

| Data Set | Precision | Recall | Accuracy | F1 | AUC(macro) | Hamming Loss |
|---|---|---|---|---|---|---|
| *top-10-code* | 0 | 0 | 0.8025 | 0 | 0.5 | 0.1974 |
| *top-50-code* | 0 | 0 | 0.9130 | 0 | 0.5 | 0.0870 |
| *top-10-category* | 0 | 0 | 0.7246 | 0 | 0.5 | 0.2753 |
| *top-50-category* | 0 | 0 | 0.8734 | 0 | 0.5 | 0.1266 |

**Table 4:** Performance with zero initialized data

## 3 Results

This section is organized as follows: baseline results are described in section **??**, performance under different configurations are described in section 3.1, and our best model performance are described in section 3.2.

### 3.1 Model Performance under Different Configurations

Different model configurations are tried to give us insight into the most appropriate model configuration. Table 5 describes the different methods of feature extraction used and the parameters tweaked. The features extracted are divided into 2 categories: non-sequential and sequential. The non-sequential features include *tfidf* and*word2vec*, which were used in Logistic Regression, Random Forest, and Feed-Forward Neural Network. The sequential features includes *wordseq* (word sequences) used in conjunction with an embedding matrix based on *word2vec*, which were used in Conv1D, RNN, LSTM, and GRU. Note that we experimented on 1) using our custom *word2vec* model created from the MIMIC III dataset and 2) on using pre-train word vectors obtained from[18]. The vector for stop words in the embedding matrix are all zeros.

Figure 3 shows the model performance of each model using different feature extraction methods pair on the *top-10-code* dataset. The raw data are also shown in the appendix (table 14 and 15). For each model, the configuration that provided the best performance here is used on the *top-50-code*, *top-10-cat*, and *top-50-cat* datasets. The results are further explained in the next section 3.2.

| Feature Extraction | Configuration | Value |
|---|---|---|
| tfidfv | feature size | 20301 - 40000 |
| | minDocFreq | 3 - 10 |
| | max_df | 0.8 - 1.0 |
| word2vec | database | self trained from MIMIC III (m3) or pre-trained from Pubmed (pm)[18] |
| | feature size | 100 - 600 |
| | pre-trained config | win 2 or win30[18] |
| wordseq | sequence length | 1500-2000 |
| | stopwords | removed from sequence or not removed |
| | embedding matrix | derived from the word2vec under different configurations |

**Table 5:** Feature Extraction Methods

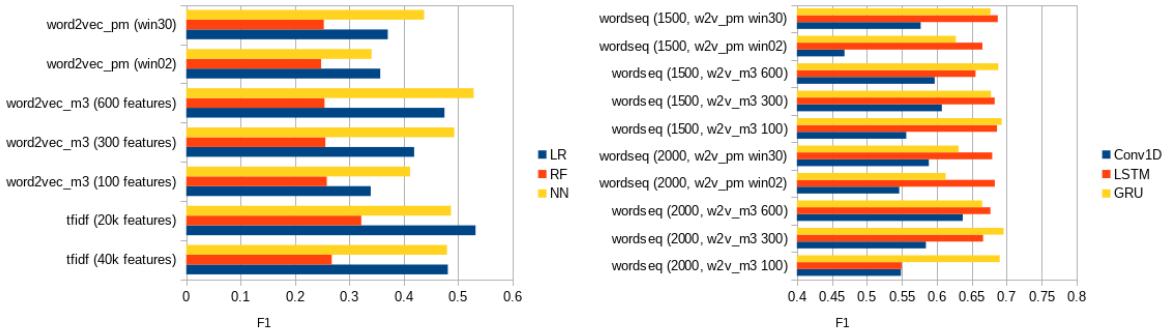


(a) Nonsequential

(b) Sequential

**Figure 3:** Model Performance under Different Configuration

For non-sequential feature extraction, *tfidf with 20000 features* gave the best f1 results for Logistic Regression and Random Forest, while *word2vec_m3 with 600 features* gave the best results for Feed-Forward Neural Networks (although *tfidfv* also gave a fairly good result for NN). In general, *tfidf* configurations generated better results than *word2vec*, probably because we are losing information. Note that the feature size for *word2vec* are at most 600 while *tfidf* is around 20,000 above.

For sequential feature extraction, *seq. length 2000 + word2vec_m3 w/ 600 features* generated the best f1 result for Conv1D, *seq. length 1500 + word2vec_pm (win30)* for LSTM, and *seq. length 2000 + word2vec_m3 w/ 300 features* for GRU. In general, all feature extraction methods generated good and comparable results for Conv1D, LSTM, and GRU. Our *word2vec* also faired well compared with the pre-trained *word2vec* models. Although not shown in figure 3(b) (but shown in table 15, the feature extraction methods were also tried for RNN, but the results were bad (0.0 - 0.23 f1 at best). This may be because the sequence length is too long (1,500 - 2,000).

## 3.2 Best Model Performance

### 3.2.1 Overview

Figure 4 and 5 shows the model performance for the *top-10-code*, *top-10-cat*, *top-50-code*, *top-50-cat* dataset (the models are ordered from best to worst, from top to bottom). Raw data are also shown in table 8, 11, 9, and 12.

For *top-10-code* and *top-10-cat*, GRU generated the best f1 results (at 0.6957 and 0.7233, respectively). In general, *top-10-cat* generated slightly better results than *top-10-code*. This makes sense because 1) we have more data per labels in *top-10-cat* and 2) the labels are less specific (the differences between labels are larger). The baseline models (Logistic Regression and Random Forest) seems to overfit the data (which can be observed from the almost 100% training results but bad test results). Feed Forward NN is not overfitting, but the results are comparable to the baseline

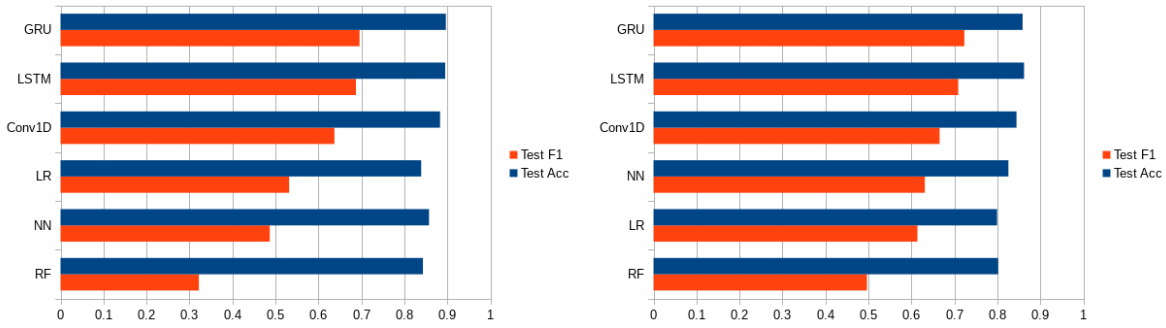


(a) top-10-code (b) top-10-cat

**Figure 4:** Model Performance Top 10

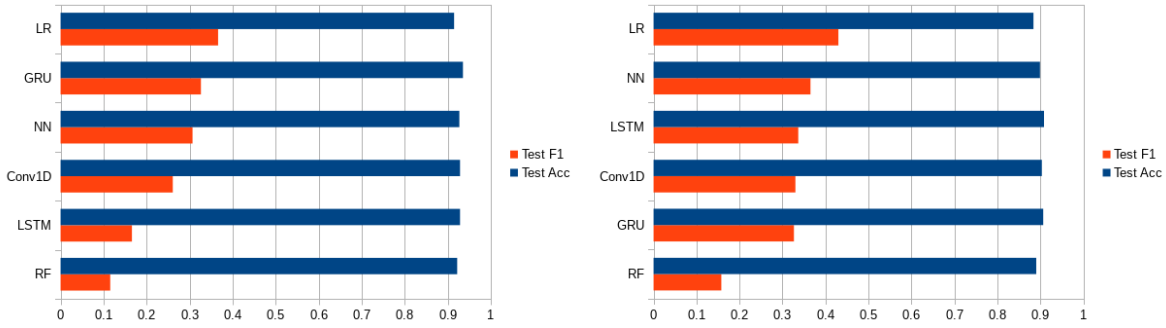


(a) top-50-code (b) top-50-cat

**Figure 5:** Model Performance Top 50

models. Conv1D produced even better results (than NN), but there are more significant improvement with LSTM and GRU (reaching around 70% f1). This signifies that our LSTM and GRU model was able to extract information from the sequence of words, otherwise lost in non-sequential feature extraction, thereby improving the f1 and also the accuracy results.

For *top-50-code* and *top-50-cat*, Logistic Regression generated the best f1 result (at 0.3662 and 0.4301, respectively). Similar to *top10*, *top-50-cat* generated slightly better results than *top-50-code*. The baseline models (Logistic Regression and Random Forest) also overfit here. However, the models that used sequential feature extraction did not produce better results (in comparison with *top10*).

### 3.2.2 Precision-Recall Curve

Table 6 shows the average of overall precision performance of our selected best performance models for GRU, LSTM and Convolution 1D. From this table, we can see that GRU generated the best precision results for *top-10-code* and *top-50-code*. Figure 6 shows precision-recall curve for the best performed models for each labels in *top-10* and the best performed 10 labels for *top-50*. The detailed class-wise precision-recall curve for the selected models are presented in Appendix H

### 3.2.3 top-50-code and top-50-cat models

Figure 7 shows a comparison between the *top-10* results and the corresponding label results (first 10) in *top-50*. For models between ICD9 codes, the first-10 results are different from the top-10 results, implying that the *top-50-code* model is unable to completely cover the *top-10-code* model capability. For models between ICD9 categories, the first-

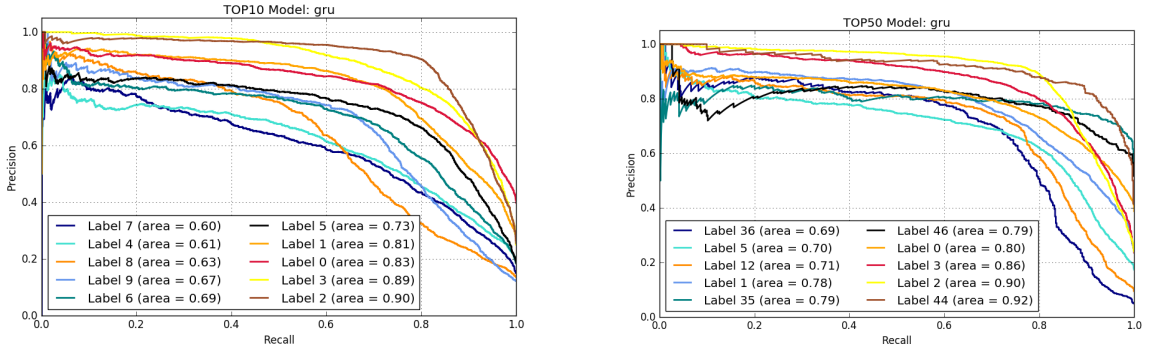


(a) top-10-code (b) top-50-code

**Figure 6:** Class-wise Precision-Recall Curve for Top 10 and Top 50

| Model | *top-10-code* | *top-10-cat* | *top-50-code* | *top-50-cat* | *top-50-code(first10)* | *top-50-cat(first10)* |
|---|---|---|---|---|---|---|
| *LSTM* | 0.7243 | 0.7915 | 0.3715 | 0.4929 | 0.7571 | 0.8426 |
| *GRU* | 0.7362 | 0.7849 | 0.4518 | 0.4792 | 0.7949 | 0.8425 |
| *Conv1D* | 0.6719 | 0.7293 | 0.3757 | 0.4565 | 0.7424 | 0.8269 |

**Table 6:** Average Precision Performance

10 results are similar to the top-10 results, implying that *top-50-cat* model is somewhat able to cover the *top-10-cat* model capability.

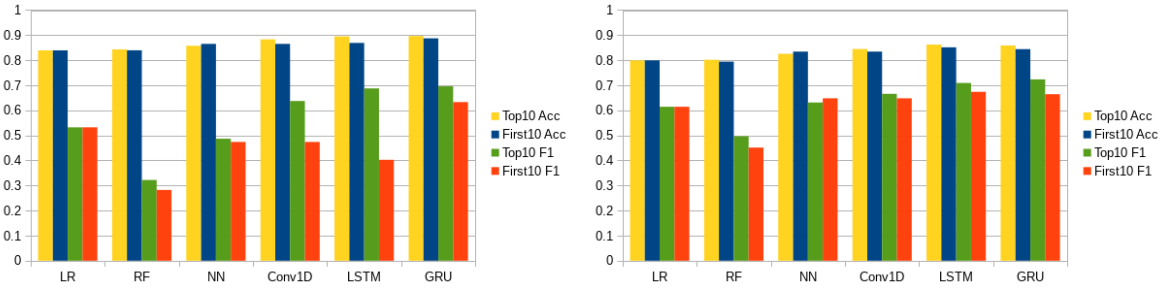


(a) top-10-code and top-50-code (first 10) (b) top-10-cat and top-50-cat (first 10)

**Figure 7:** Top 10 vs Top 50 (first 10)

### 3.2.4 Results Comparison

Prakash and Zhao[5] use bag-of-words from discharge notes and Condensed Memory Neural Network (C-MemNN) to tackle the similar problem as we do. They tested their algorithm with top 50 and top 100 labels under metrics such as macro AUC, average precision over the top five predictions, and hamming loss. In order to compare our work with theirs, We calculated the same metrics for our best performed models for top 50 codes, and the results are listed in Table 7.

From this comparison, we can see that our work outperformed on macro AUC and top 5 precision for top 50 codes. Their hamming loss is significantly better than ours. We believe that our word2vec representation plus memory network will make further progress on this problem.

| Model | AUC (macro) | Precision @5 | Hamming Loss |
|---|---|---|---|
| *C-MemNN (Prakash)* | 0.833 | 0.42 | **0.01** |
| *GRU (our)* | **0.8599** | **0.8109** | 0.0645 |
| *LSTM (our)* | 0.8298 | 0.8054 | 0.0714 |
| *Conv1D (our)* | 0.8302 | 0.7998 | 0.0714 |

**Table 7:** Performance comparison with reference[5]

## 4 Conclusion

In this study, we applied deep learning based natural language processing frameworks to automatically assign clinical ICD-9 codes from free-text clinical notes. We compared different models and feature extraction methods, effectively establishing a strong benchmark for NLP in the MIMIC III dataset. We designed and produced deep learning models for predicting the top 10 ICD9 codes and categories which were better than our baseline models (best F1 results: 69.57% GRU to 53.20% Logistic Regression, and 72.33% GRU to 63.13% Feed Forward Neural Network, respectively). Top 50 ICD9 codes and categories results were not outperformed to our baseline (32.63% GRU to 36.62% Logistic Regression, and 33.67% GRU to 36.51% Feed Forward Neural Network, respectively). Even though our best model performance is around 70% F1, we hope our implementation and evaluation of the current state-of-the-art algorithms can serve as a baseline for further research on this topic.

## 5 Future Work

Our current models for top 50 ICD9 codes and categories were not as successful. This can be because our current model design lacks ”capability” in effectively distinguishing between 50 different labels. To improve our model capability, we can increase our neural network neurons (node count and layers), which greatly increases computation requirements / training time. Another approach is to produce 5 *top-10* models in parallel (each model predicting 10 labels), thereby making our *top-50* models have the same model capability as our *top-10* models, but also increasing computation requirements / training time by 5 times. Figure 8 shows the result of trying this approach for Conv1D using the *top-50-code* dataset. The parallel approach did improve F1 from 0.2609 to 0.3879, but to obtain *top-10-code*-level F1(0.6373), more samples (occurrences) for labels 11 to 50 is needed.

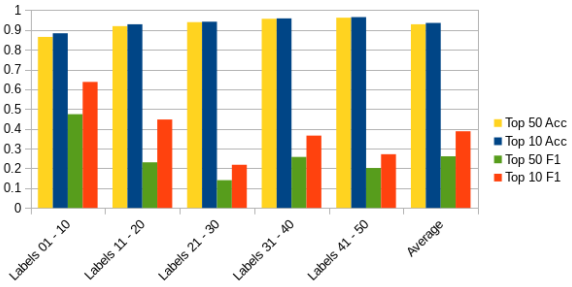


**Figure 8:** Parallel Top 10 vs Top 50

Our custom *word2vec* model used CBOW. We didn't have the chance to try skip-gram (although the pre-trained *word2vec* are skip-gram based). Some previous studies say that skip-gram outperforms CBOW in biomedical domain tasks[18]. Therefore in future work, we would like to see how the different *word2vec* parameters affect our ICD9 code or category classifier.

Further research on what words affect the probability of a prediction the most in our baseline models could improve our understanding of the relationship between symptoms and diagnosis. This could change our preprocessing and feature extraction methods and ultimately improve our deep learning models. Also, further analysis of the labels our model successfully classified vs labels unsuccessfully classified can give us deeper insight about the classification problem (e.g.: whether additional data will improve our results, whether some disease are just harder to classify).

As discussed in Section 3.2.4, we are also interested in exploring more on memory networks and combining it with

our input features.

## References


1. Ashly D Black, Josip Car, Claudia Pagliari, Chantelle Anandan, Kathrin Cresswell, Tomislav Bokun, Brian McKinstry, Rob Procter, Azeem Majeed, and Aziz Sheikh. The impact of ehealth on the quality and safety of health care: a systematic overview. *PLoS Med*, 8(1):e1000387, 2011.

2. Edward Choi, Mohammad Taha Bahadori, and Jimeng Sun. Doctor ai: Predicting clinical events via recurrent neural networks. *arXiv preprint arXiv:1511.05942*, 2015.

3. Zachary C Lipton, David C Kale, Charles Elkan, and Randall Wetzell. Learning to diagnose with lstm recurrent neural networks. *arXiv preprint arXiv:1511.03677*, 2015.

4. Ping Chen, Araly Barrera, and Chris Rhodes. Semantic analysis of free text and its application on automatically assigning icd-9-cm codes to patient records. In *Cognitive Informatics (ICCI), 2010 9th IEEE International Conference on*, pages 68–74. IEEE, 2010.

5. Aaditya Prakash, Siyuan Zhao, Sadid A Hasan, Vivek Datla, Kathy Lee, Ashequl Qadir, Joey Liu, and Oladimeji Farri. Condensed memory networks for clinical diagnostic inferencing. *arXiv preprint arXiv:1612.01848*, 2016.

6. F Martin-Sanchez, K Verspoor, et al. Big data in medicine is driving big changes. *Yearb Med Inform*, 9(1):14–20, 2014.

7. John P Pestian, Christopher Brew, Paweł Matykiewicz, Dj J Hovermale, Neil Johnson, K Bretonnel Cohen, and Włodzisław Duch. A shared task involving multi-label classification of clinical free text. In *Proceedings of the Workshop on BioNLP 2007: Biological, Translational, and Clinical Language Processing*, pages 97–104. Association for Computational Linguistics, 2007.

8. MBA Ira Goldstein and MLS Anna Arzumtsyan. Three approaches to automatic assignment of icd-9-cm codes to radiology reports. 2007.

9. Laritza M Rodriguez and Dina Demner Fushman. Automatic classification of structured product labels for pregnancy risk drug categories, a machine learning approach. In *AMIA Annual Symposium Proceedings*, volume 2015, page 1093. American Medical Informatics Association, 2015.

10. Ben J Marafino, Jason M Davies, Naomi S Bardach, Mitzi L Dean, R Adams Dudley, and John Boscardin. N-gram support vector machines for scalable procedure and diagnosis classification, with applications to clinical free text data from the intensive care unit. *Journal of the American Medical Informatics Association*, 21(5):871–875, 2014.

11. Vijay Garla, Caroline Taylor, and Cynthia Brandt. Semi-supervised clinical text classification with laplacian svms: an application to cancer case management. *Journal of biomedical informatics*, 46(5):869–875, 2013.

12. Adam Wright, Allison B McCoy, Stanislav Henkin, Abhivyakti Kale, and Dean F Sittig. Use of a support vector machine for categorizing free-text notes: assessment of accuracy across two institutions. *Journal of the American Medical Informatics Association*, 20(5):887–890, 2013.

13. Adler Perotte, Rimma Pivovarov, Karthik Natarajan, Nicole Weiskopf, Frank Wood, and Noémie Elhadad. Diagnosis code assignment: models and evaluation metrics. *Journal of the American Medical Informatics Association*, 21(2):231–237, 2014.

14. Priyanka Nigam. Applying deep learning to icd-9 multi-label classification from medical records. pages 1–8.

15. MIMIC-III, a freely accessible critical care database. *Scientific data*, 3:160035, 2016.

16. Tomas Mikolov, Kai Chen, Greg Corrado, and Jeffrey Dean. Efficient estimation of word representations in vector space. *CoRR*, abs/1301.3781, 2013.

17. Tomas Mikolov, Ilya Sutskever, Kai Chen, Greg Corrado, and Jeffrey Dean. Distributed representations of words and phrases and their compositionality. In *Proceedings of the 26th International Conference on Neural Information Processing Systems*, NIPS'13, pages 3111–3119, USA, 2013. Curran Associates Inc.

18. Billy Chiu, Gamal Crichton, Anna Korhonen, and Sampo Pyysalo. How to Train Good Word Embeddings for Biomedical NLP. *Proceedings of the 15th Workshop on Biomedical Natural Language Processing*, pages 166–174, 2016.

19. Grigorios Tsoumakas and Ioannis Katakis. Multi-label classification: An overview. *International Journal of Data Warehousing and Mining*, 3(3), 2006.

20. Chuan Yu Foo Yifan Mai Caroline Suen Adam Coates Andrew Maas Awni Hannun Brody Huval Tao Wang Sameep Tandon Andrew Ng, Jiquan Ngiam. UFLDL Tutorial. http://ufldl.stanford.edu/tutorial/supervised/FeatureExtractionUsingConvolution/, 2008. [Online; accessed 18-April-2017].

21. Wen-tau Yih, Kristina Toutanova, John C Platt, and Christopher Meek. Learning discriminative projections for text similarity measures. In *Proceedings of the Fifteenth Conference on Computational Natural Language Learning*, pages 247–256. Association for Computational Linguistics, 2011.

22. Yelong Shen, Xiaodong He, Jianfeng Gao, Li Deng, and Grégoire Mesnil. Learning semantic representations using convolutional neural networks for web search. In *Proceedings of the 23rd International Conference on World Wide Web*, pages 373–374. ACM, 2014.

23. Yoon Kim. Convolutional neural networks for sentence classification. *arXiv preprint arXiv:1408.5882*, 2014.

24. Min-Ling Zhang and Zhi-Hua Zhou. A review on multi-label learning algorithms. *IEEE transactions on knowledge and data engineering*, 26(8):1819–1837, 2014.

# Appendices

## A Model Performance for Top 10 Label Codes

| | Training | | | | Test | | | |
|---|---|---|---|---|---|---|---|---|
| Model | Precision | Recall | Accuracy | F1 | Precision | Recall | Accuracy | F1 |
| Logistic Regression | 0.9564 | 0.9440 | 0.9786 | 0.9501 | 0.5801 | 0.4934 | 0.8392 | 0.5320 |
| Random Forest | 0.9989 | 0.6988 | 0.9501 | 0.8086 | 0.7573 | 0.2340 | 0.8432 | 0.3219 |
| Feed Forward NN | 0.7768 | 0.5041 | 0.8879 | 0.5763 | 0.6703 | 0.4193 | 0.8575 | 0.4868 |
| Conv1D | 0.8312 | 0.6713 | 0.9165 | 0.7371 | 0.7408 | 0.5687 | 0.8832 | 0.6373 |
| LSTM RNN | 0.8106 | 0.6971 | 0.9154 | 0.7445 | 0.7574 | 0.6380 | 0.8950 | 0.6874 |
| GRU RNN | 0.7936 | 0.6971 | 0.9126 | 0.7397 | 0.7502 | 0.6519 | 0.8967 | 0.6957 |

**Table 8:** Model Performance for *top-10-code*

## B Model Performance for Top 50 Codes

| | Training | | | | Test | | | |
|---|---|---|---|---|---|---|---|---|
| Model | Precision | Recall | Accuracy | F1 | Precision | Recall | Accuracy | F1 |
| Logistic Regression | 0.9863 | 0.9768 | 0.9945 | 0.9815 | 0.4372 | 0.3213 | 0.9148 | 0.3662 |
| Random Forest | 0.9985 | 0.2852 | 0.9451 | 0.3866 | 0.5377 | 0.0953 | 0.9220 | 0.1155 |
| Feed Forward NN | 0.9636 | 0.5542 | 0.9640 | 0.6892 | 0.5773 | 0.2335 | 0.9271 | 0.3067 |
| Conv1D | 0.6085 [a] | 0.2663 | 0.9365 | 0.3200 [a] | 0.4792 [a] | 0.2169 | 0.9286 | 0.2609 [a] |
| LSTM RNN | 0.3526 [a] | 0.1642 | 0.9325 | 0.1891 [a] | 0.4022 [a] | 0.1445 | 0.9286 | 0.1659 [a] |
| GRU RNN | 0.6539 [a] | 0.3433 | 0.9460 | 0.3947 [a] | 0.5592 [a] | 0.2782 | 0.9354 | 0.3263 [a] |

**Table 9:** Model Performance for *top-50-code*

| | Training | | | | Test | | | |
|---|---|---|---|---|---|---|---|---|
| Model | Precision | Recall | Accuracy | F1 | Precision | Recall | Accuracy | F1 |
| Logistic Regression | 0.9564 | 0.9440 | 0.9786 | 0.9501 | 0.5801 | 0.4934 | 0.8392 | 0.5320 |
| Random Forest | 0.9946 | 0.4937 | 0.9110 | 0.6305 | 0.7869 | 0.2009 | 0.8395 | 0.2822 |
| Feed Forward NN | 0.9347 | 0.8037 | 0.9580 | 0.8589 | 0.7674 | 0.5837 | 0.9062 | 0.6486 |
| Conv1D | 0.7708 | 0.4673 | 0.8858 | 0.5377 | 0.6784 | 0.4109 | 0.8650 | 0.4739 |
| LSTM RNN | 0.6204[a] | 0.3829 | 0.8805 | 0.4348[a] | 0.5748 | 0.3526 | 0.8688 | 0.4025[a] |
| GRU RNN | 0.8351 | 0.6474 | 0.9168 | 0.7181 | 0.7520 | 0.5618 | 0.8871 | 0.6328 |

**Table 10:** Model Performance for *top-50-code* (first 10)

[a] result contained $nan$. Computed by replacing $nan$ with zero.

## C Model Performance for Top 10 Label Categories

| | Training | | | | Test | | | |
|---|---|---|---|---|---|---|---|---|
| Model | Precision | Recall | Accuracy | F1 | Precision | Recall | Accuracy | F1 |
| Logistic Regression | 0.9437 | 0.9309 | 0.9652 | 0.9372 | 0.6458 | 0.5856 | 0.7994 | 0.6141 |
| Random Forest | 0.9983 | 0.8134 | 0.9500 | 0.8954 | 0.7653 | 0.3801 | 0.8019 | 0.4966 |
| Feed Forward NN | 0.7978 | 0.6575 | 0.8655 | 0.7147 | 0.7243 | 0.5689 | 0.8257 | 0.6313 |
| Conv1D | 0.8039 | 0.6637 | 0.8681 | 0.7128 | 0.7613 | 0.6126 | 0.8446 | 0.6657 |
| LSTM RNN | 0.8146 | 0.6807 | 0.8749 | 0.7343 | 0.7926 | 0.6536 | 0.8622 | 0.7090 |
| GRU RNN | 0.8150 | 0.7613 | 0.8909 | 0.7861 | 0.7580 | 0.6941 | 0.8588 | 0.7233 |

**Table 11:** Model Performance for *top-10-cat*

## D Model Performance for Top 50 Label Categories

| | Training | | | | Test | | | |
|---|---|---|---|---|---|---|---|---|
| Model | Precision | Recall | Accuracy | F1 | Precision | Recall | Accuracy | F1 |
| Logistic Regression | 0.9750 | 0.9572 | 0.9887 | 0.9659 | 0.4858 | 0.3894 | 0.8841 | 0.4301 |
| Random Forest | 0.9986 | 0.3294 | 0.9277 | 0.4465 | 0.6568 | 0.1142 | 0.8906 | 0.1576 |
| Feed Forward NN | 0.9613 | 0.5488 | 0.9473 | 0.6853 | 0.6298 | 0.2773 | 0.8992 | 0.3651 |
| Conv1D | 0.7428 | 0.3262 | 0.9163 | 0.3870 | 0.5635 [a] | 0.2770 | 0.9035 | 0.3301 [a] |
| LSTM RNN | 0.7117 [a] | 0.3363 | 0.9194 | 0.3804 [a] | 0.5869 | 0.2945 | 0.9087 | 0.3367 [a] |
| GRU RNN | 0.6695 [a] | 0.3227 | 0.9179 | 0.3726 [a] | 0.5611 [a] | 0.2809 | 0.9067 | 0.3266 [a] |

**Table 12:** Model Performance for *top-50-cat*

| | Training | | | | Test | | | |
|---|---|---|---|---|---|---|---|---|
| Model | Precision | Recall | Accuracy | F1 | Precision | Recall | Accuracy | F1 |
| Logistic Regression | 0.9437 | 0.9309 | 0.9652 | 0.9372 | 0.6458 | 0.5856 | 0.7994 | 0.6141 |
| Random Forest | 0.9937 | 0.6321 | 0.8999 | 0.7687 | 0.7877 | 0.3282 | 0.7944 | 0.4512 |
| Feed Forward NN | 0.7873 | 0.6425 | 0.8811 | 0.7031 | 0.7730 | 0.6267 | 0.8724 | 0.6878 |
| Conv1D | 0.7945 | 0.6652 | 0.8670 | 0.7142 | 0.7296 | 0.5979 | 0.8345 | 0.6481 |
| LSTM RNN | 0.7963 | 0.6863 | 0.8768 | 0.7213 | 0.7515 | 0.6362 | 0.8514 | 0.6738 |
| GRU RNN | 0.7901 | 0.6803 | 0.8729 | 0.7213 | 0.7382 | 0.6196 | 0.8442 | 0.6641 |

**Table 13:** Model Performance for *top-50-cat* (first 10)

[a] result contained $nan$. Computed by replacing $nan$ with zero.

## E Model Performance under Different Configurations (Non Sequential)

| Model | Configuration | Feature | Precision | Recall | Accuracy | F1 |
|---|---|---|---|---|---|---|
| Logistic Regression | Iter=25 | tfidf (40k features) | 0.5290 | 0.4445 | 0.8232 | 0.4810 |
| Logistic Regression | Iter=10 | tfidf (20k features) | 0.5801 | 0.4934 | 0.8392 | 0.5320 |
| Logistic Regression | Iter=50 | word2vec_m3 (100 features) | 0.5820 | 0.2682 | 0.8353 | 0.3393 |
| Logistic Regression | Iter=100 | word2vec_m3 (300 features) | 0.6265 | 0.3388 | 0.8448 | 0.4191 |
| Logistic Regression | Iter=100 | word2vec_m3 (600 features) | 0.6467 | 0.3914 | 0.8513 | 0.4749 |
| Logistic Regression | Iter=100 | word2vec_pm (win02) | 0.5938 | 0.2807 | 0.8340 | 0.3568 |
| Logistic Regression | Iter=75 | word2vec_pm (win30) | 0.6030 | 0.2921 | 0.8370 | 0.3706 |
| Random Forest | Depth=30 | tfidf (40k features) | 0.7529 | 0.1881 | 0.8354 | 0.2676 |
| Random Forest | Depth=30 | tfidf (20k features) | 0.7573 | 0.2340 | 0.8432 | 0.3219 |
| Random Forest | Depth=20 | word2vec_m3 (100 features) | 0.5281 | 0.1907 | 0.8233 | 0.2585 |
| Random Forest | Depth=20 | word2vec_m3 (300 features) | 0.5471 | 0.1866 | 0.8237 | 0.2559 |
| Random Forest | Depth=20 | word2vec_m3 (600 features) | 0.5296 | 0.1857 | 0.8228 | 0.2543 |
| Random Forest | Depth=20 | word2vec_pm (win02) | 0.5420 | 0.1794 | 0.8224 | 0.2480 |
| Random Forest | Depth=20 | word2vec_pm (win30) | 0.5283 | 0.1852 | 0.8225 | 0.2530 |
| Feed Forward NN | nn_model_1 | tfidf (40k features) | 0.6975 | 0.3785 | 0.8542 | 0.4795 |
| Feed Forward NN | nn_model_2 | tfidf (20k features) | 0.6703 | 0.4193 | 0.8575 | 0.4868 |
| Feed Forward NN | nn_model_2 | word2vec_m3 (100 features) | 0.5429 | 0.3505 | 0.8304 | 0.4116 |
| Feed Forward NN | nn_model_2 | word2vec_m3 (300 features) | 0.5467 | 0.4627 | 0.8329 | 0.4929 |
| Feed Forward NN | nn_model_2 | word2vec_m3 (600 features) | 0.5737 | 0.4972 | 0.8406 | 0.5285 |
| Feed Forward NN | nn_model_2 | word2vec_pm (win02) | 0.5426 | 0.2778 | 0.8377 | 0.3408 |
| Feed Forward NN | nn_model_4 | word2vec_pm (win30) | 0.5228 | 0.3856 | 0.8253 | 0.4375 |

**Table 14:** Model Performance under Different Configurations (Non Sequential)

[a]result contained $nan$. Computed by replacing $nan$ with zero.

## F Model Performance under Different Configurations (Sequential)

| Model | Configuration | Seq. Length | Embedding Matrix | Precision | Recall | Accuracy | F1 |
|---|---|---|---|---|---|---|---|
| Conv1D | conv1d_6 | 2000 | w2v_m3 (100 features) | 0.7460 | 0.4626 | 0.8758 | 0.5489 |
| Conv1D | conv1d_6 | 2000 | w2v_m3 (300 features) | 0.7492 | 0.5103 | 0.8779 | 0.5846 |
| Conv1D | conv1d_6 | 2000 | w2v_m3 (600 features) | 0.7408 | 0.5687 | 0.8832 | 0.6373 |
| Conv1D | conv1d_6 | 2000 | w2v_pm (win02) | 0.6424 | 0.4962 | 0.8642 | 0.5464 |
| Conv1D | conv1d_6 | 2000 | w2v_pm (win30) | 0.7283 | 0.5217 | 0.8757 | 0.5888 |
| Conv1D | conv1d_6 | 1500 | w2v_m3 (100 features) | 0.7304 | 0.4851 | 0.8744 | 0.5565 |
| Conv1D | conv1d_6 | 1500 | w2v_m3 (300 features) | 0.7141 | 0.5443 | 0.8762 | 0.6074 |
| Conv1D | conv1d_6 | 1500 | w2v_m3 (600 features) | 0.7578 | 0.5081 | 0.8805 | 0.5972 |
| Conv1D | conv1d_6 | 1500 | w2v_pm (win02) | 0.5635 [a] | 0.2770 | 0.9035 | 0.3301 [a] |
| Conv1D | conv1d_6 | 1500 | w2v_pm (win30) | 0.6819 | 0.5323 | 0.8658 | 0.5771 |
| RNN | rnn_2 | 2000 | w2v_m3 (100 features) | 0.1772 [a] | 0.0758 | 0.8067 | 0.08693 [a] |
| RNN | rnn_2 | 2000 | w2v_m3 (300 features) | 0.2291 [a] | 0.0476 | 0.8067 | 0.06774 [a] |
| RNN | rnn_2 | 2000 | w2v_m3 (600 features) | 0.1110 [a] | 0.0513 | 0.8052 | 0.0702 [a] |
| RNN | rnn_2 | 2000 | w2v_pm (win02) | 0.0000 [a] | 0.0000 | 0.8025 | 0.0000 [a] |
| RNN | rnn_2 | 2000 | w2v_pm (win30) | 0.0000 [a] | 0.0000 | 0.8025 | 0.0000 [a] |
| RNN | rnn_2 | 1500 | w2v_pm (win02) | 0.1150 [a] | 0.0390 | 0.8045 | 0.0535 [a] |
| RNN | rnn_2 | 1500 | w2v_pm (win30) | 0.1087 [a] | 0.0545 | 0.8025 | 0.0630 [a] |
| LSTM | lstm_1 | 2000 | w2v_m3 (100 features) | 0.6857 | 0.4958 | 0.8749 | 0.5499 |
| LSTM | lstm_1 | 2000 | w2v_m3 (300 features) | 0.7577 | 0.6001 | 0.8922 | 0.6664 |
| LSTM | lstm_1 | 2000 | w2v_m3 (600 features) | 0.7287 | 0.6381 | 0.8901 | 0.6768 |
| LSTM | lstm_1 | 2000 | w2v_pm (win02) | 0.7464 | 0.6381 | 0.8931 | 0.6831 |
| LSTM | lstm_1 | 2000 | w2v_pm (win30) | 0.7529 | 0.6288 | 0.8939 | 0.6794 |
| LSTM | lstm_1 | 1500 | w2v_m3 (100 features) | 0.7275 | 0.6523 | 0.8910 | 0.6862 |
| LSTM | lstm_1 | 1500 | w2v_m3 (300 features) | 0.7566 | 0.6281 | 0.8948 | 0.6829 |
| LSTM | lstm_1 | 1500 | w2v_m3 (600 features) | 0.7549 | 0.5974 | 0.8908 | 0.6556 |
| LSTM | lstm_1 | 1500 | w2v_pm (win02) | 0.7702 | 0.5984 | 0.8930 | 0.6654 |
| LSTM | lstm_1 | 1500 | w2v_pm (win30) | 0.7574 | 0.6380 | 0.8950 | 0.6874 |
| GRU | gru_4 | 2000 | w2v_m3 (100 features) | 0.7456 | 0.6486 | 0.8953 | 0.6902 |
| GRU | gru_4 | 2000 | w2v_m3 (300 features) | 0.7502 | 0.6519 | 0.8967 | 0.6957 |
| GRU | gru_4 | 2000 | w2v_m3 (600 features) | 0.7395 | 0.6164 | 0.8893 | 0.6651 |
| GRU | gru_4 | 2000 | w2v_pm (win02) | 0.7166 | 0.5572 | 0.8804 | 0.6128 |
| GRU | gru_4 | 2000 | w2v_pm (win30) | 0.7577 | 0.5672 | 0.8868 | 0.6313 |
| GRU | gru_4 | 1500 | w2v_m3 (100 features) | 0.7475 | 0.6514 | 0.8955 | 0.6930 |
| GRU | gru_4 | 1500 | w2v_m3 (300 features) | 0.7758 | 0.6111 | 0.8967 | 0.6776 |
| GRU | gru_4 | 1500 | w2v_m3 (600 features) | 0.7557 | 0.6389 | 0.8955 | 0.6881 |
| GRU | gru_4 | 1500 | w2v_pm (win02) | 0.7228 | 0.5773 | 0.8815 | 0.6273 |
| GRU | gru_4 | 1500 | w2v_pm (win30) | 0.7404 | 0.6277 | 0.8907 | 0.6769 |

**Table 15:** Model Performance under Different Configurations (Sequential)

[a] result contained $nan$. Computed by replacing $nan$ with zero.

## G Best Performance Model Architectures

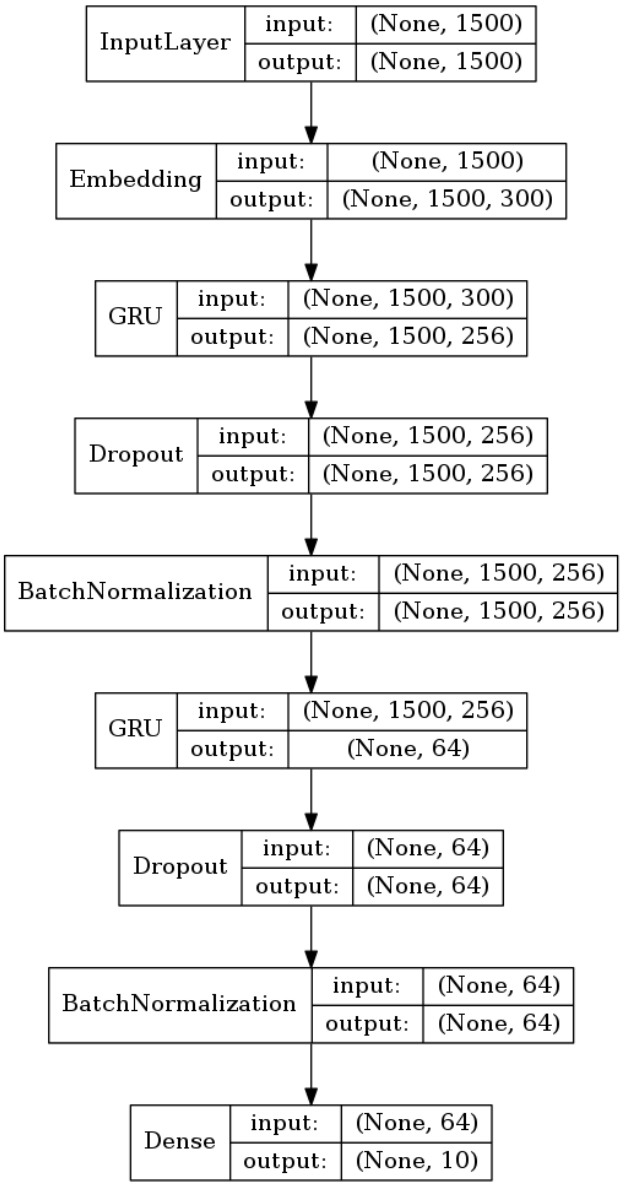


**Figure 9:** Best GRU Model Architecture for Top 10 Codes, Top 50 Codes, Top 10 Categories, and Top 50 Categories

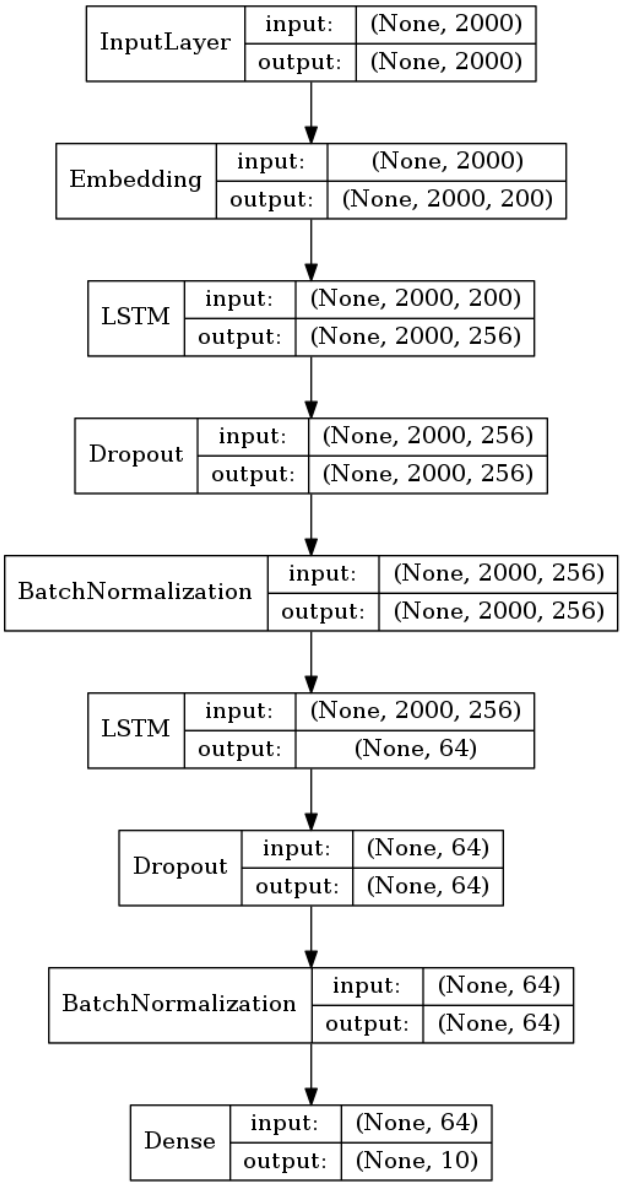


**Figure 10:** Best LSTM Model Architecture for Top 10 Codes, Top 50 Codes, Top 10 Categories, and Top 50 Categories

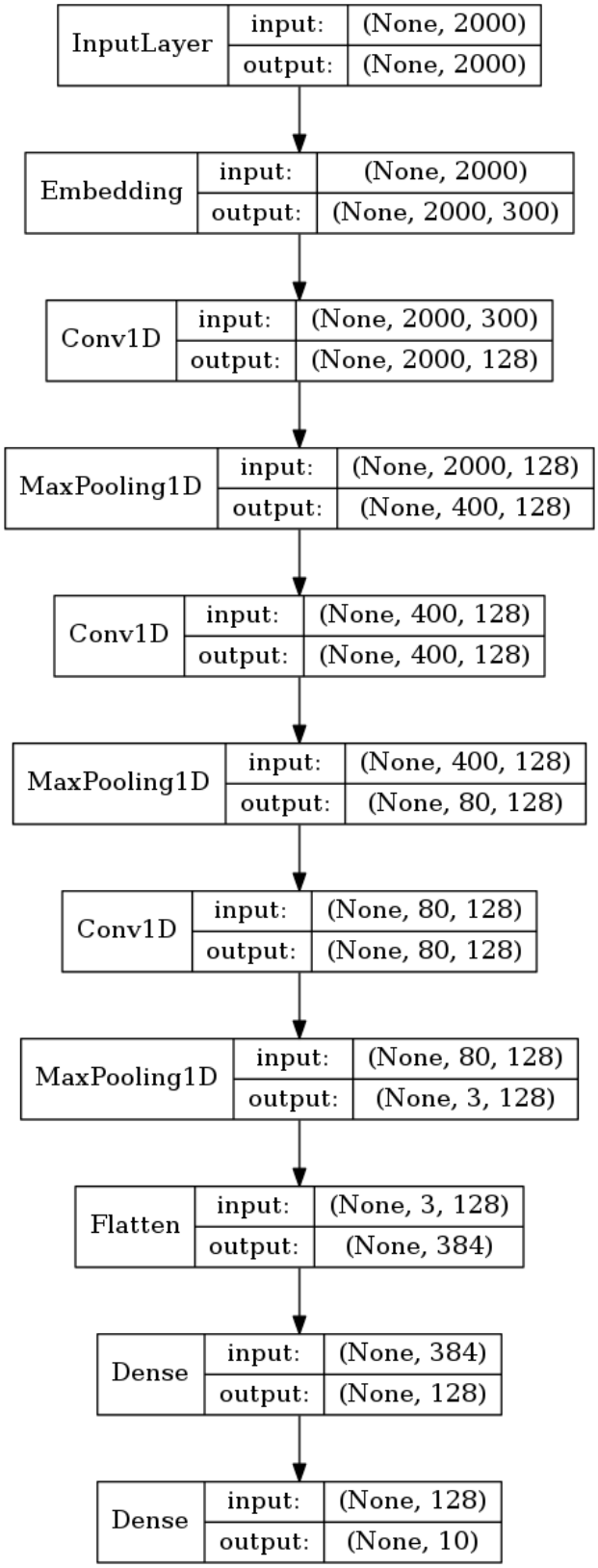


**Figure 11:** Best Convolution 1D Model Architecture for Top 10 Codes and Top 10 Categories

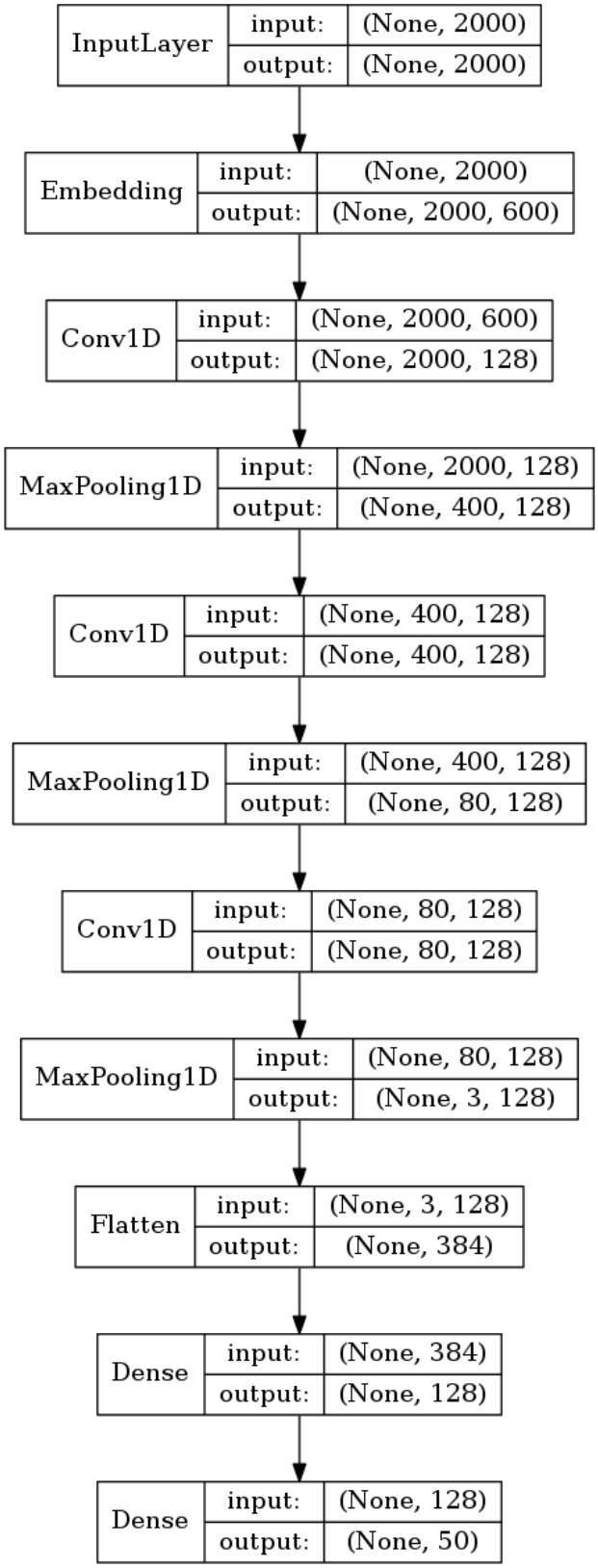


**Figure 12:** Best Convolution 1D Model Architecture for Top 50 Codes and Top 50 Categories

## H Best Performance Models (LSTM, GRU, Conv1D) Precision-Recall Curve

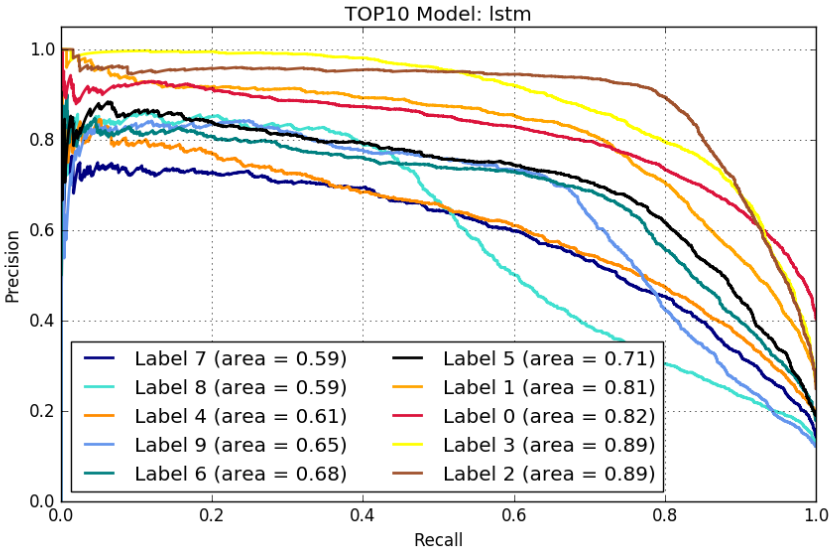


**Figure 13:** Precision-Recall Curve for Top 10 Codes under LSTM Model

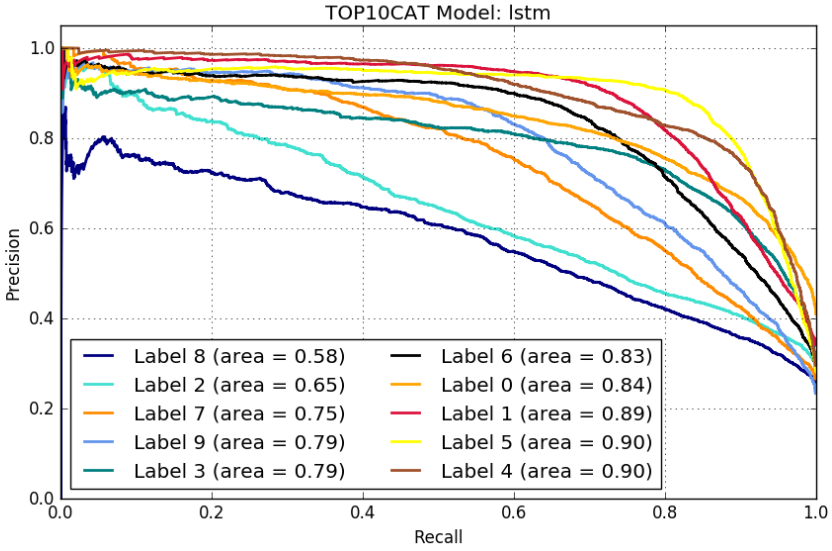


**Figure 14:** Precision-Recall Curve for Top 10 Categories under LSTM Model

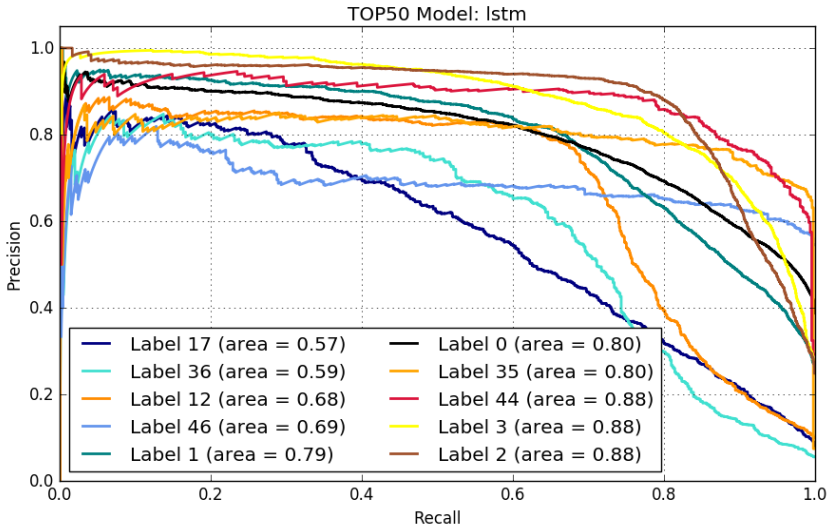


**Figure 15:** Precision-Recall Curve for Top 50 Codes under LSTM Model

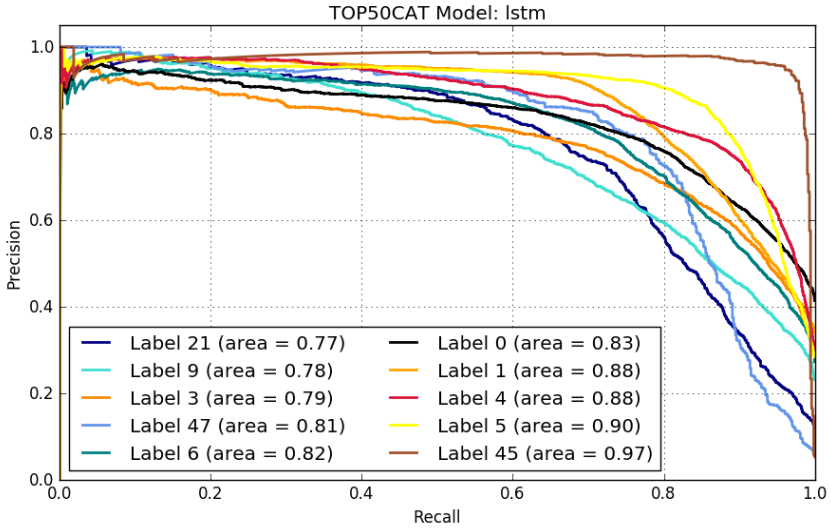


**Figure 16:** Precision-Recall Curve for Top 50 Categories under LSTM Model

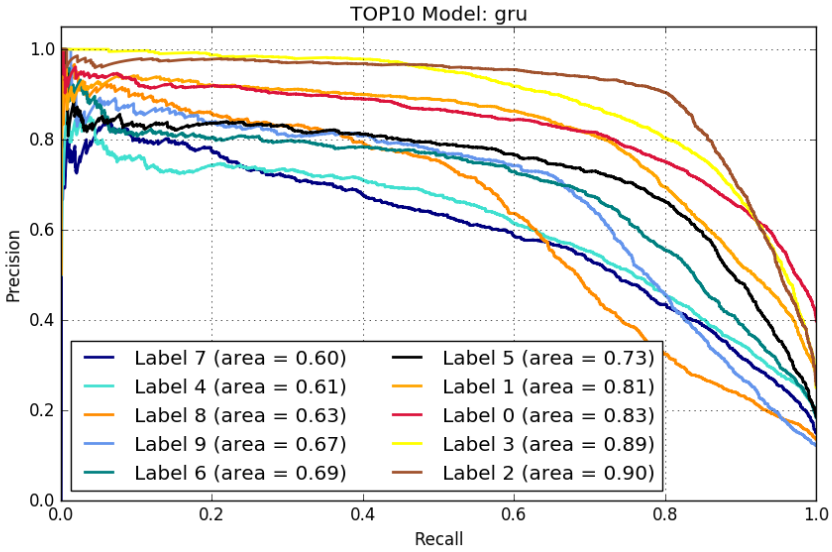


**Figure 17:** Precision-Recall Curve for Top 10 Codes under GRU Model

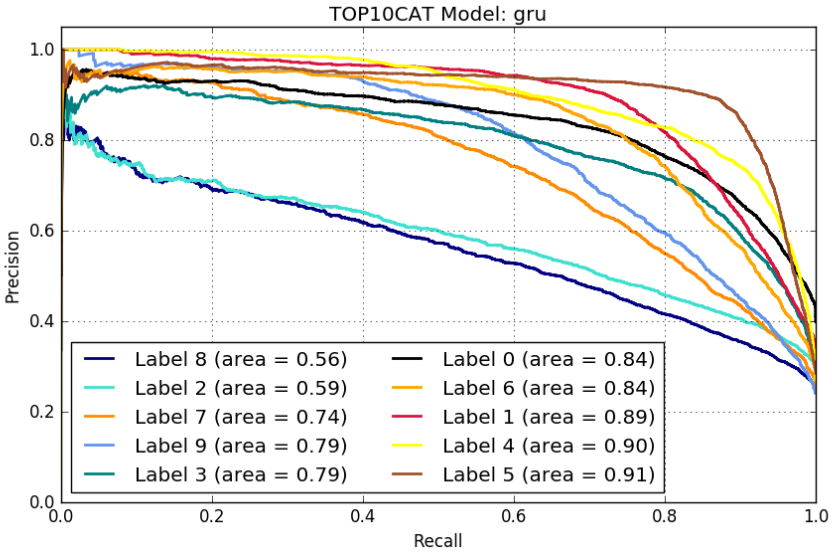


**Figure 18:** Precision-Recall Curve for Top 10 Categories under GRU Model

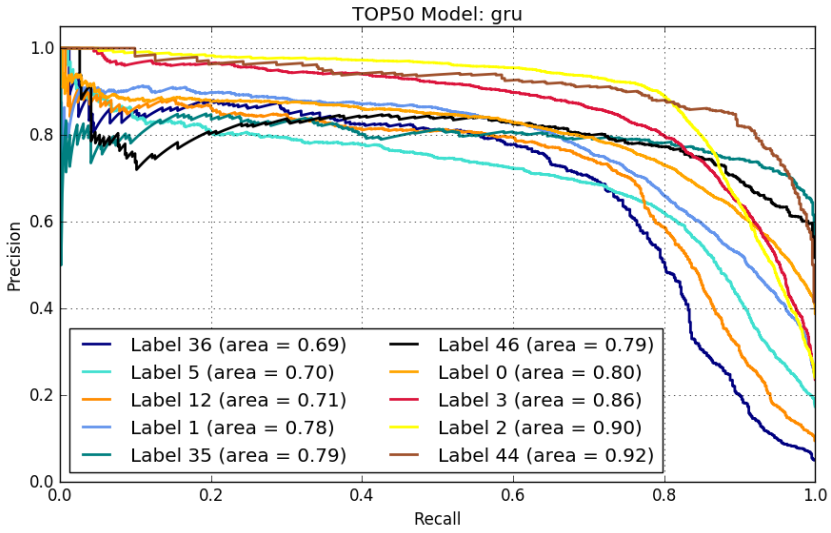


**Figure 19:** Precision-Recall Curve for Top 50 Codes under GRU Model

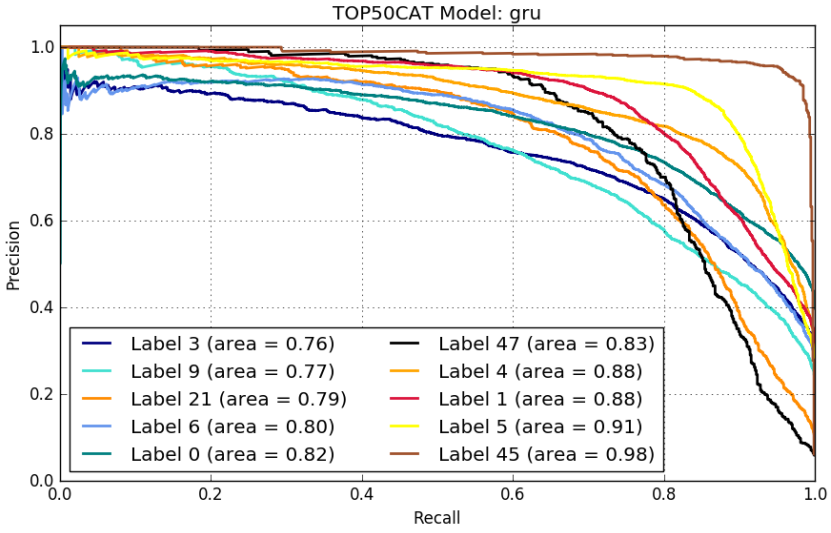


**Figure 20:** Precision-Recall Curve for Top 50 Categories under GRU Model

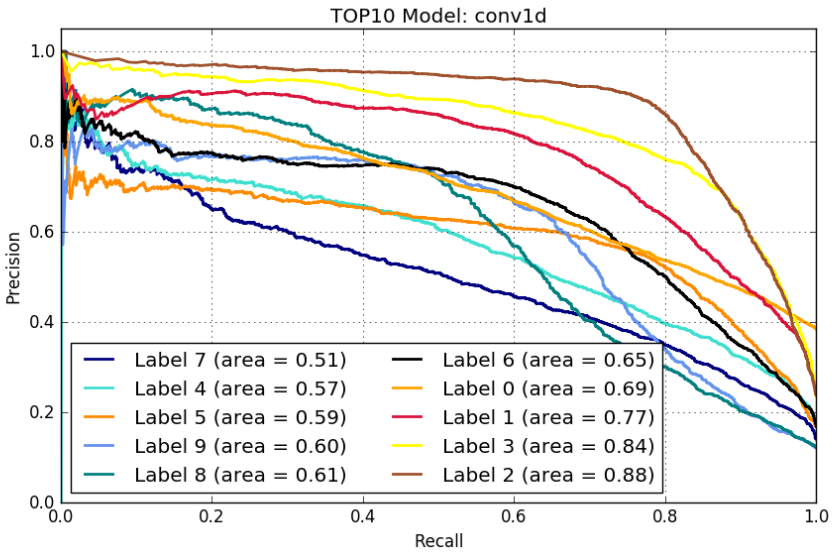


**Figure 21:** Precision-Recall Curve for Top 10 Codes under Convolution 1D Model

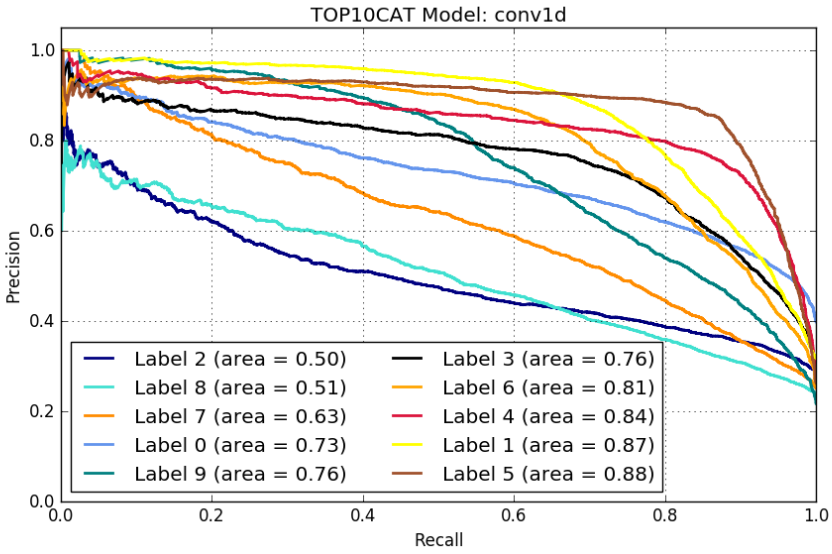


**Figure 22:** Precision-Recall Curve for Top 10 Categories under Convolution 1D Model

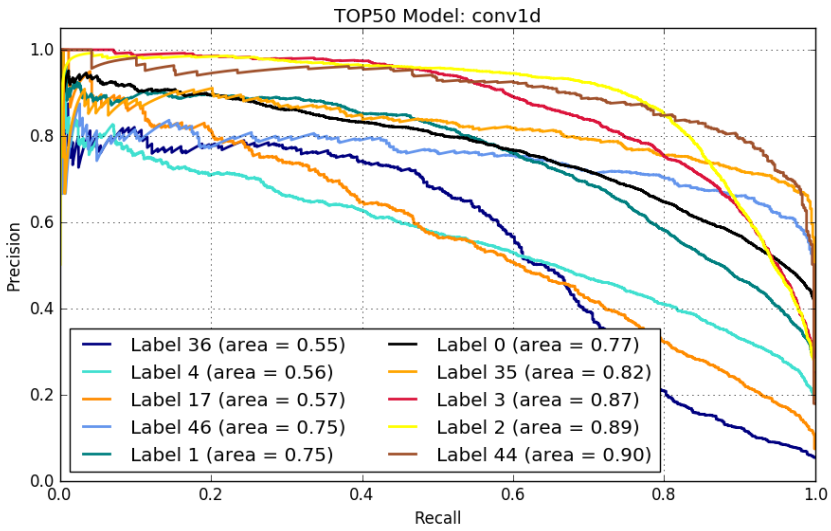


**Figure 23:** Precision-Recall Curve for Top 50 Codes under Convolution 1D Model

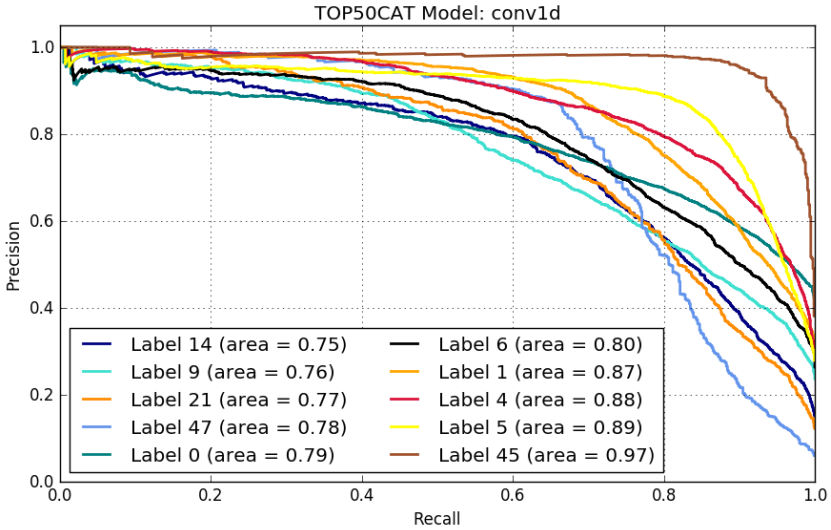


**Figure 24:** Precision-Recall Curve for Top 50 Categories under Convolution 1D Model